

<https://doi.org/10.1038/s44303-026-00150-1>

# Advanced imaging techniques for tumor intraoperative navigation imaging

Ke Li<sup>1,2</sup>, Yiyin Zhang<sup>1,2</sup>, Houpu Yang<sup>1</sup> & Shu Wang<sup>1</sup> ✉

Cancer remains a leading cause of mortality and morbidity, with surgical resection being a fundamental element of treatment. However, early detection and precise tumor resection are critical for improving survival and minimizing recurrence. Conventional imaging techniques face limitations in resolution, real-time feedback, and tissue differentiation, often leading to imprecise resection. Recent advancements in intraoperative imaging technologies have gradually addressed these challenges. Fluorescence imaging offers superior tissue penetration, enhanced signal-to-noise ratio, and resilience under a surgical environment, making it ideal for real-time tissue and lymph node detection. Targeted molecular probes and advanced fluorescence techniques further enhance tumor specificity. Modalities like photoacoustic and Raman spectroscopy provide complementary insights, while three-dimensional reconstruction and multimodal systems improve anatomical precision. Early clinical studies demonstrate these technologies' high sensitivity and clinical feasibility in tumor detection and margin assessment. Integrating artificial intelligence and personalized medicine into intraoperative imaging holds promise for further refining these techniques, leading to more tailored and effective interventions. This review provides an overview of the evolution and clinical practice of novel intraoperative imaging technologies, highlighting their superiority over traditional methods and outlining the future research directions in this rapidly advancing field.

## Requirements and challenges in intraoperative navigation

According to the latest statistics from the International Agency for Research on Cancer in 2024, nearly 20 million new cancer cases and ~9.7 million cancer-related deaths occurred in 2022<sup>1</sup>. These figures underscore cancer's immense burden on public health, highlighting the critical need for effective prevention, early detection, and treatment strategies on a global scale. In the meantime, tumors are the leading cause of death after acute cardiovascular events<sup>2</sup>, emphasizing the critical need for enhanced management approaches. Early-stage tumor screening and surgical resection are the main interventions to reduce tumor mortality, with the latter being a primary therapeutic approach. Tumor resection relies on the surgeon's experience and the outcomes of preoperative imaging diagnostics to guide decision-making. Complete tumor resection with minimal damage to surrounding healthy tissues is crucial for reducing recurrence rates and improving overall prognosis.

Intraoperative imaging plays a pivotal role in guiding these procedures. Conventional imaging techniques, such as ultrasound, magnetic resonance imaging (MRI), computed tomography (CT), and

positron emission tomography (PET), have been widely used for intraoperative guidance. But they often face limitations in resolution, real-time feedback, and tissue differentiation. Impacting the diagnosis and determination of tumor extent is crucial, yet many of these technologies are inconvenient for intraoperative manipulation. Moreover, conventional imaging tools are often cumbersome and impractical for dynamic intraoperative settings. Present shortcomings, such as limited spatial resolution, slow imaging speed, and shallow penetration depths, hinder their utility in achieving optimal surgical outcomes<sup>3</sup>, often resulting in incomplete tumor resection and a higher risk of recurrence<sup>4</sup>.

Consequently, such cutting-edge imaging modalities are indispensable for the precise delineation of tumor margins, which is critical in facilitating targeted surgical procedures and optimizing patient outcomes<sup>5</sup>. This review is dedicated to assessing the clinical potential and translational impact of novel intraoperative imaging technologies (Fig. 1), with a particular emphasis on those that surpass the constraints of traditional imaging methods, thereby enhancing the precision of surgical interventions.

<sup>1</sup>Department of Breast Center, Peking University People's Hospital, Peking University, Beijing, China. <sup>2</sup>These authors contributed equally: Ke Li, Yiyin Zhang.

✉ e-mail: [shuwang@pkuph.edu.cn](mailto:shuwang@pkuph.edu.cn)

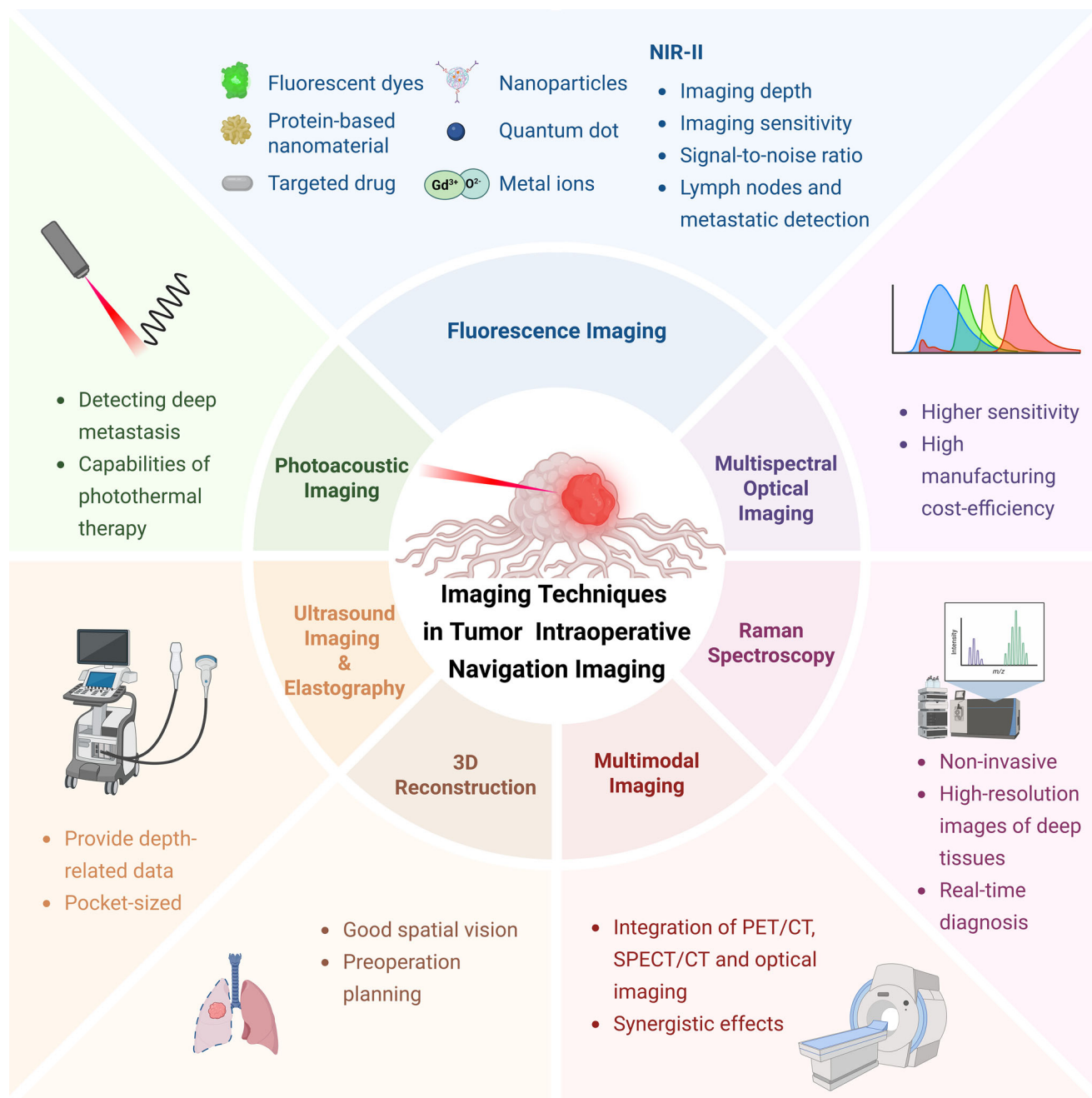


**Fig. 1 | Advanced imaging techniques for intraoperative navigation imaging.** CT computed tomography, NIR near infrared, PET positron emission tomography, SPECT single-photon emission computed tomography, 3D three-dimensional.

## Imaging strategies in tumor resection surgery

### Fluorescence imaging: from general to targeted approaches

**Traditional fluorescence imaging.** Fluorescence molecular imaging, utilizing fluorescent dyes that selectively target tumors, has gained substantial attention for its application in detecting tumors during surgical procedures and in the staging of cancer<sup>6</sup>. Currently approved non-targeted fluorescent imaging agents by the US. The US Food and Drug Administration (FDA) includes indocyanine green (ICG), methylene blue (MB), fluorescein sodium, 5-aminolevulinic acid (5-ALA), and hexaminolevulinate, which are widely used for perfusion assessment, angiography, and metabolic fluorescence-guided procedures (Table 1).

ICG is commonly used in fluorescence imaging, for it is a near-infrared (NIR) dye that has been extensively used for tumor visualization due to its favorable fluorescence properties and relatively low toxicity. Building upon

the established benefits of ICG fluorescence imaging, several studies have underscored its efficacy a range of cancer, establishing its role in intraoperative navigation.

For normal application, it can effectively delineate tumor boundaries in tumors such as breast cancer<sup>7</sup>, bone and soft tissue sarcoma surgeries<sup>8</sup>, and aids in identifying early-stage lung cancer with a high detection rate<sup>9</sup>. It also enhances the accuracy of sentinel lymph node biopsy in gastric cancer by visualizing lymphatic vessels and nodes with only 0.1 mg/ml concentration<sup>10</sup>, improving surgical precision. These studies collectively highlight the versatility and reliability of ICG in fluorescence-guided surgery across various tumor types. At low concentrations, ICG offers high contrast and real-time feedback, significantly improving surgical outcomes while maintaining strong safety and practicality. However, ICG's utility is limited by its shallow tissue penetration, which impedes the detection of deep-

**Table 1 | FDA-approved fluorescent imaging agents**

Agent	Trade name(s)	Type	Wavelength (Exc/Em)	Mechanism	FDA-approved Indication(s)	Approval year
Indocyanine green (ICG)	IC-GREEN®, SPY Agent Green™, etc.	Non-targeted NIR dye	~780/805 nm	Passive distribution	Fluorescence imaging of blood flow, tissue perfusion, lymphatic mapping, and biliary tract visualization	1959
Methylene blue (MB)	ProvyBlue®	Non-targeted visible and NIR dye	~665 nm	Passive distribution	Approved as injectable dye/contrast agent; widely used in clinical fluorescence imaging applications (off-label)	2016
Fluorescein sodium	Fluorescite®, etc.	Non-targeted visible-light dye	~465/520 nm	Passive distribution	Fluorescein angiography/angiography (ophthalmic vascular imaging)	2006
5-Aminolevulinic acid HCl (5-ALA)	Gleolan®	Metabolic activatable dye	Blue excitation/red PpIX emission	Metabolic conversion to PpIX	Visualization of malignant tissue in suspected high-grade glioma during surgery	2017
Hexaminolevulinate HCl (HAL)	Cysview®, Hexivix®, etc.	Metabolic activatable dye	Blue excitation/red PpIX fluorescence	Local conversion to protoporphyrin IX	Cystoscopic optical imaging for the detection of non-muscle invasive bladder cancer	2010
Patofolicanine sodium (OTL-38)	CYTALUX®	Targeted molecular fluorescent agent (FRα)	~785/800 nm	Small-molecule ligand targeting folate receptor-α (FRα)	(1) Intraoperative identification of malignant lesions in ovarian cancer; (2) Intraoperative visualization of pulmonary lesions in known or suspected lung cancer	2021 (ovary), 2023 (lung)
Pegulicanine	LUMISIGHT™	Activatable molecular imaging agent	NIR	Protease-activated peptide probe	Detection of residual cancer tissue in breast-conserving surgery (lumpectomy)	2024

Em Emission, etc et cetera, Exc Excitation, NIR near infrared ray, PpIX protoporphyrin IX.

seated tumors or those with low solid components, such as ground-glass nodules in lung cancer<sup>9</sup>. Additionally, ICG's efficacy varies according to tumor characteristics, with limited uptake in tumors that are predominantly ground-glass opacities.

**Enhancing specificity in fluorescent imaging: targeted novel probes and ligands.** To overcome the limitations of traditional fluorescent dyes, targeted probes have been developed by targeting proteins. The characteristics of tumor-associated proteins and the expression differences between tissues are extremely important for the type and evolution of tumors. Since nearly 50% East Asians with lung cancer, especially non-small-cell lung cancer, carry the *EGFR* mutation<sup>11</sup>, a new epidermal growth factor receptor (EGFR)-targeted fluorescence imaging technology has been developed for the intraoperative determination of lung cancer<sup>12</sup>, which can rapidly identify tumor boundaries and metastatic lymph nodes during surgery, providing high sensitivity and specificity. Similarly, human epidermal growth factor receptor 2 (HER2) overexpression in 20–25% of breast cancers has led to the development of monoclonal antibody-conjugated NIR fluorescent dyes, such as trastuzumab and pertuzumab conjugated with IRDye800, which exhibit high specificity for HER2-positive breast cancer cells and tissues, and hold promise for fluorescence-guided surgery<sup>13</sup>.

In recent years, with more attention paid to some new tumor antigens, molecular probes targeting these antigens have been gradually developed. Trophoblast cell surface antigen 2 (TROP2) is significantly overexpressed on the cell surface of more than 85% of tumors<sup>14</sup>, including breast cancer, with a marked differential expression between malignant cells and normal cells, making it a viable target for diagnostic imaging probes. The FDA-approved antibody-drug conjugate sacituzumab govitecan, which targets TROP2, has also been conjugated with ICG to enable precise tumor identification in breast cancer<sup>15</sup>. Similarly, developing probes targeting B7H3, an immune checkpoint protein overexpressed in osteosarcoma, allows for highly accurate labeling of tumor regions, even in metastatic lesions<sup>16</sup>. Additionally, the c-MET receptor has emerged as a target for fluorescence imaging in penile squamous cell carcinoma<sup>17</sup>, and ICG conjugated with the tumor-targeting peptide p28 has shown promise in breast cancer surgeries<sup>18</sup>; these modifications help in reducing positive margins and minimizing recurrence. It is further proved that a good tracer can not only ensure the safety of patients, but also provide good imaging during surgery, especially the image of the tumor margin.

Furthermore, when these dyes are coupled with relevant drugs, they pave the way for innovative image-guided therapeutic strategies. For instance, the use of cetuximab conjugated with IRDye800CW in head and neck cancer surgeries has demonstrated its ability to effectively bind to EGFR-overexpressing tumors<sup>19</sup>, providing enhanced contrast for tumor margin identification. A study has also been conducted to assess the practicality of using intraoperative fluorescence imaging with bevacizumab-800CW in endoscopic transsphenoidal surgery for pituitary neuroendocrine tumors<sup>20</sup>. They discovered that this approach was clinically well-tolerated and provided the most effective differentiation between tumor tissue and the surrounding healthy tissue among all the dosages investigated<sup>20</sup>. Nonetheless, given the widespread expression of many proteins across various tissues, the accuracy of future optical imaging techniques will necessitate the identification of more specific protein markers or the integration of additional physicochemical characteristics of tumor tissues.

Despite these advances, challenges remain, such as potential non-specific binding and the need for more refined protein markers to enhance imaging accuracy. To address this, probes targeting the tumor micro-environment and its unique characteristics have been developed, offering improved specificity and detection capabilities. Given that the tumor microenvironment possesses both commonalities and specificities across different tumor types, fluorescent probes targeting the tumor micro-environment are a research hotspot. For example, a CREKA-GK8-QC probe<sup>21</sup>, designed to target fibronectin and activated by metalloproteinases,

has been developed for breast cancer imaging, enhancing the detection of primary tumors and micro-metastases, and facilitating the complete removal of cancerous tissues. The probe's activation by metalloproteinases ensures specificity within the tumor microenvironment<sup>21</sup>. Combining ICG with human serum albumin plays an important role in laparoscopic anatomical liver resection, and has provided enhanced fluorescence imaging of hepatic segments<sup>4,22</sup>. Another research explored the cathepsin-activatable imaging agent AKRO-6qICG in ex vivo scenarios<sup>23</sup>. This revealed a 100% sensitivity and negative predictive value for detecting tumor-positive margins via near-infrared fluorescence imaging. A further innovation is the use of an NIR-II fluorescence probe IR1080<sup>24</sup>, which allows ICG to bind covalently to albumin in the bloodstream. This binding enhances brightness and stability and enables targeted detection of micro-metastases through albumin-binding proteins overexpressed in tumor environments<sup>24</sup>. A novel hypoxia-activatable fluorescent probe has been developed for tumor imaging, capitalizing on the hypoxic nature of tumor environments to enhance imaging specificity<sup>25</sup>.

Comparative studies have shown that antibody fragments, such as urokinase plasminogen activator receptor (uPAR)-targeting antibody fragments<sup>26</sup>, can visualize tumor sites earlier while maintaining good fluorescence intensity, striking an optimal balance between imaging resolution and speed of detection. This significantly enhances the detection and resection of sentinel lymph nodes in breast cancer patients. At the expense of peak fluorescence intensity, uPAR-targeting antibody fragments achieved earlier tumor visualization in fluorescence-guided surgery.

On the basis of targeting specific proteins, more probes have been designed to adapt to the multivariate imaging environment. For example, a modification involves stabilizing ICG with alpha-lactalbumin to form gold quantum clusters<sup>27</sup>. These clusters provide multifunctional imaging capabilities, including fluorescence, CT, and MRI, which enhance long circulation times as well<sup>28</sup>. ICG fluorescence imaging can also combine with <sup>99m</sup>Tc-prostate-specific membrane antigen-targeted radio-guided surgery workflow for primary prostate cancer surgery<sup>28</sup>.

To date, the FDA has approved two targeted molecular fluorescent probes—pafolacianine, which targets folate receptor- $\alpha$ , and pegulicianine, an activatable protease-responsive probe—for intraoperative molecular imaging (Table 1). Recent studies have demonstrated their efficacy in various cancer surgeries. For instance, a phase III study of pafolacianine for ovarian cancer resection showed that it significantly improved the identification of additional cancer lesions not detected by traditional methods such as palpation or white light, with a sensitivity of 83% and a patient false-positive rate of 24.8%<sup>29</sup>. Similarly, the ELUCIDATE trial focused on lung cancer, reported that pafolacianine successfully identified occult lesions, including synchronous cancers, with a sensitivity of 76.9% and a false-positive rate of 25.9%<sup>30,31</sup>. Additionally, in breast cancer surgeries, pegulicianine fluorescence-guided surgery (pFGS) reduced the need for re-excision by 19% among patients who underwent excision of pFGS-guided shaves<sup>31</sup>. The sensitivity of pFGS for identifying residual tumor in lumpectomy cavities was 76.3%<sup>31</sup>, while its specificity was 85.2%<sup>32</sup>.

#### Advancements and challenges of fluorescence lifetime imaging.

Beyond advancements in probe design, improvements in imaging techniques also contribute to the precise intraoperative identification of tumors. Fluorescence lifetime (FLT) imaging, which measures the time a fluorescent molecule spends in its excited state following laser excitation, provides a significant advantage over traditional intensity-based imaging. It measures the average time a molecule spends in its excited state following laser excitation, offering a distinct advantage over traditional intensity-based imaging by providing a photophysical parameter that is largely independent of excitation power, probe concentration, and tissue uptake<sup>33–35</sup>. FLT is unaffected by the concentration of the fluorescent molecules or the intensity of the excitation light, thus providing a higher signal-to-noise ratio. It also enables the acquisition of relevant information about the tumor microenvironment.

FLT imaging significantly enhanced tumor contrast in preclinical models of human breast cancer when an EGFR antibody was labeled with a near-infrared fluorophore, demonstrating improved sensitivity and specificity compared to traditional intensity-based imaging<sup>35</sup>. It can also provide cellular-level tumor specificity in patients injected with an EGFR-targeted near-infrared fluorescent probe, showcasing the potential for accurate tumor delineation and cancer-specific molecular expression detection in vivo<sup>34</sup>. Furthermore, a recent first-in-human study demonstrated that after systemic ICG administration, the FLT of tumor tissue is consistently and significantly longer than that of adjacent normal tissue across a wide spectrum of solid tumors, enabling tumor-normal discrimination with accuracies exceeding 97% and sensitivities and specificities above 90%<sup>33</sup>. Its robustness against measurement conditions and its potential for absolute quantification across different imaging systems, some challenges accompany its implementation<sup>35</sup>.

FLT imaging has shown remarkable promise in improving tumor contrast and providing more accurate tumor delineation, even in cases of complex tissue compositions. Unlike intensity-based fluorescence, FLT is independent of excitation power, probe concentration, and tissue optical heterogeneity, resulting in substantially improved signal-to-noise ratios and robust tumor contrast even in the presence of strong nonspecific dye accumulation. However, implementing FLT imaging faces challenges, particularly due to the limited availability of FDA-approved time-domain imaging systems and the higher cost compared to continuous-wave (CW) systems. Despite these hurdles, the consistent enhancement in tumor contrast and the potential for multiplexed imaging using FLT technology suggest that FLT imaging is expected to play a significant role in improving tumor detection and precision during cancer surgery as the technology matures.

**Advanced nanomaterials in fluorescence imaging.** With the development of technology, more and more nanomaterials have been developed. Recent studies have demonstrated the utility of real-time fluorescence imaging using ICG and <sup>99m</sup>Tc nanocolloid tracers in bilateral sentinel lymph node mapping for vulvar cancer<sup>3</sup>, with ICG showing a satisfactory detection rate and potential to minimize operative complications. Gd<sub>2</sub>O<sub>3</sub> nanoparticles combined with radiopharmaceuticals have also been utilized for triple-excited fluorescence imaging and image-guided surgery, significantly improving optical signal intensity and tissue penetration depth<sup>36</sup>. This enhancement allows for better visualization of tumor margins during surgery, thereby improving the accuracy of tumor resections. Targeting the tumor microenvironment is also an effective strategy for nanomaterials.

Interestingly, targeted fluorescent probe delivery is not limited to injection, but also includes very simple methods, such as spray. A novel fluorescent nanoprobe, Poly-g-BAT<sup>37</sup>, has been developed for colorectal cancer imaging. This nanoprobe allows for both intravenous injection and topical spraying<sup>37</sup>. These kinds of innovations are expanding the applications of fluorescence imaging, and also increasing the convenience of clinical use and reducing injection injury. Small molecule probes conjugated with dyes, an emerging area of research, have highlighted their potential for targeted tumor imaging and improved specificity.

**Shifting from NIR-I to NIR-II.** Advancements in NIR imaging have led to a clearer distinction between the NIR-I (700–900 nm) and NIR-II (900–1880 nm) spectral regions<sup>38</sup>. Recent research has highlighted the advantages of NIR-II imaging, particularly in deep tissue penetration and sensitivity.

NIR-II imaging provides improved contrast at depths of several centimeters due to reduced tissue autofluorescence, lower photon scattering, and decreased photon absorption at longer wavelengths<sup>5,39,40</sup>. Multiple studies have demonstrated that NIR-II imaging has higher spatial resolution and improved signal-to-noise ratio, which means better differentiation between tumors and surrounding tissues is allowed, and it becomes more feasible to detect small features within tissues<sup>5,39</sup>. Since both NIR-I and NIR-

II imaging possess the capability for real-time imaging, their compatibility with operating room lighting is a significant consideration. Unlike NIR-I imaging, which necessitates low lighting to prevent interference, NIR-II imaging can be conducted under bright lighting conditions<sup>5,39</sup>. It has also been found that NIR-II imaging showed a significantly higher tumor-to-normal-tissue ratio in patients with intrahepatic metastasis<sup>39</sup>. However, this conclusion has only been verified in a small number of tumor types, and more extensive conclusions need further clinical validation.

In the field of lymph node (LN)-invaded cancer detection, the significant ability to suppress photon scattering and exhibit zero autofluorescence seems more important, since LNs have a smaller margin and need more accuracy. At the same time, fluorescent agents with higher brightness should also be explored. Studies have also explored the use of ultrabright quantum dots, such as PbS/CdS core/shell nanoparticles, which outperform ICG in terms of brightness and photostability, requiring only picomolar doses for sentinel lymph node detection<sup>41</sup>. This reduction in required dosage will also be applied to intraoperative imaging of clinical patients with lower toxicity.

Overall, NIR-II imaging offers superior imaging depth, imaging sensitivity, signal-to-noise ratio, and the adaptability of the surgical environment, making it particularly advantageous for detecting deep tumors, lymph nodes, and metastatic lesions. While the imaging depth and quality of NIR-II hold great promise, there is currently a lack of clinically available experimental probes. Continued efforts to develop and translate these probes into clinical practice are essential for realizing the full potential of NIR-II fluorescence imaging.

### Photoacoustic imaging

Photoacoustic imaging (PAI) combines the strengths of both optical and acoustic signals, offering enhanced penetration capabilities that are particularly advantageous for deep-tissue imaging. By swiftly adjusting the excitation light to various wavelengths, PAI facilitates *in vivo* mapping of a wide array of chromophores. This includes endogenous substances, such as hemoglobin, myoglobin, melanin, water, lipids, and nucleic acids, as well as exogenous agents, such as targeting probes. Importantly, this imaging process is achieved without relying on ionizing radiation, heavy-metal contrast agents, or necessitating specialized radiation shielding facilities<sup>42</sup>.

By leveraging the depth-sensing prowess of acoustic waves combined with the contrast-rich characteristics of light, PAI has shown exceptional promise in detecting early-stage tumors, as well as in detecting distant micro-metastases with high sensitivity. For instance, PAI has been shown to detect hepatic micro-metastases from melanoma as small as 400  $\mu\text{m}$ , outperforming traditional imaging modalities such as ultrasound and MRI, demonstrating its value in early cancer detection<sup>43</sup>. Employing advanced photoacoustic-specific probes, such as copper sulfide nanoparticles<sup>44</sup> or reversibly switchable bacterial phytochromes like BphP1<sup>45</sup>, has revolutionized multi-scale photoacoustic tomography. These probes substantially augment the penetration depth and detection sensitivity, thereby enabling more precise imaging of tumors and metastases<sup>44,45</sup>.

By detecting endogenous and exogenous biomarkers within the tumor microenvironment and leveraging complementary strengths when integrated with other imaging modalities, PAI enables precise delineation of tumor boundaries and provides surgeons with comprehensive, real-time information during resection. In addition to ICG, a growing number of clinically evaluated photoacoustic probes, including small-molecule dye-conjugated agents currently in clinical trials, further expand the applicability of PAI<sup>46</sup>, enhancing both detection sensitivity and molecular specificity. Together, these advancements support more accurate tumor removal while maximally preserving healthy tissue.

### Multispectral imaging and hyperspectral imaging

Multispectral imaging (MSI) offers detailed tissue characteristic information, crucial for distinguishing malignant from healthy cells during surgery. By integrating multiple spectral bands, MSI optimizes photon contribution and enriches informational content, enhancing tissue diversity visualization.

This capability significantly reduces surgical uncertainties and enhances intraoperative precision. MSI's unique advantage in intraoperative imaging, combining spectral specificity and multi-band synthesis, outperforms NIR and PAI imaging in certain applications, providing more comprehensive intraoperative navigation.

Unlike NIR imaging, which often employs single fluorescent dye signals with limited spectral data, hampering the differentiation of complex tissues, and PAI, primarily dependent on absorption spectra for specific molecules with a restricted range, MSI excels by leveraging multiple spectral bands spanning from visible to near-infrared light. This capability enables MSI to discern minute molecular variations within tissues, yielding high-resolution, precise imaging. It effectively captures a wide array of molecular traits, thus offering a more comprehensive and detailed imaging approach. A breakthrough in MSI technology is the development of bioinspired imaging systems, such as the hexachromatic camera modeled after the mantis shrimp's visual system<sup>47</sup>. By fully leveraging all six channels, this camera synergizes diagnostic data with inherently coregistered morphological details. Another innovation inspired by the Morpho butterfly's compound eye integrates spectral tapetal filters with photodetectors on a single chip, achieving 1000 times higher sensitivity and 7 times better spatial co-registration accuracy compared to existing clinical imaging systems<sup>48</sup>. These bioinspired designs provide high manufacturing cost-efficiency, making detailed and accurate image information more accessible for clinical use.

Moreover, MSI has also demonstrated exceptional performance in detecting multiple targets with high precision. For example, the multispectral fluorescence imaging probes Nimotuzumab-ICG and Atezolizumab-Cy5.5 used in MSI showed remarkable detection accuracy for oral squamous cell carcinoma<sup>49</sup>. The sensitivity and specificity of Nimotuzumab-ICG were 96.4% and 100%, respectively, while for Atezolizumab-Cy5.5, they were 95.2% and 88.9%. Its potential in distinguishing multiple markers makes it ideal for intraoperative navigation in scenarios involving multiple targets and molecules, particularly in resource-limited settings.

Hyperspectral imaging (HSI), while similar to MSI, captures a much broader range of wavelengths, including both visible and near-infrared spectra. HSI systems capture spectral data at each pixel within an image, enabling precise tissue differentiation.

A study using NIR-HSI in gastrointestinal stromal tumor detection showed 91.3% sensitivity and 73% specificity, identifying deep lesions missed by traditional imaging<sup>50</sup>. When using HSI to identify cervical intraepithelial neoplasia (CIN) lesions in the cervix, 95% sensitivity and 96% specificity were achieved, with spectral data from 555 to 585 nm effectively differentiating CIN from normal tissue<sup>51</sup>. In breast cancer surgeries, HSI demonstrated 95% sensitivity and 96% specificity in distinguishing malignant from normal breast tissue using spectral data from 420 to 620 nm, improving intraoperative tumor detection and margin assessment accuracy<sup>52</sup>.

Whereas MSI enables rapid and broad tissue discrimination through a limited set of spectral bands, HSI delivers richer molecular information across an expanded spectral range, thereby offering enhanced capability for accurate tissue characterization. MSI is highly effective for quick procedures like tumor resection, while HSI excels in identifying early-stage cancers and complex tissue variations, albeit at the cost of longer data processing times.

### Ultrasound imaging and elastography

In contrast to fluorescence imaging, which is primarily effective for assessing spatial extent and superficial tissue information, ultrasound imaging can provide depth-related data that is crucial for understanding tumor infiltration into deeper tissues. Real-time acquisition of 3D ultrasound images can assist surgeons in identifying blood vessels and tumor boundaries more accurately, leading to enhanced safety and precision in tumor resection. One notable application involves the use of geometrically variable 3D ultrasound for mechanically assisted image-guided therapy during focal liver tumor ablation, enhancing applicator guidance and placement verification<sup>53</sup>. This system has the potential to improve applicator placement and reduce local

cancer recurrence by improving applicator placement during interventional procedures.

Furthermore, elastography ultrasound is capable of evaluating tissue stiffness, effectively distinguishing tumors from healthy tissues, and expanding the scope of clinical application. A study presented a virtual elastography ultrasound (V-EUS) via a generative adversarial network for breast cancer diagnosis<sup>54</sup>. V-EUS improved the diagnostic performance of pocket-sized ultrasound devices by ~5%. Despite the lack of significant differences in diagnostic accuracy between V-EUS and traditional high-end ultrasound<sup>54</sup>, this finding highlights the promise of virtual elastography ultrasound in delivering precise diagnostic outcomes for tumors situated in deeper tissues and in upgrading the functionality of portable ultrasound devices to include elastography imaging capabilities.

### Raman spectroscopy

Raman spectroscopy, an optical detection method based on the inelastic scattering of light by vibrating molecules, has garnered significant attention due to its ability to provide molecular chemical information. This technique reveals detailed chemical information of complex biological samples and is characterized by its non-invasive nature, high sensitivity, and specificity<sup>55</sup>. Unlike other imaging techniques, such as fluorescence or NIR, which rely on exogenous contrast agents, Raman spectroscopy can offer endogenous molecular information without the need for exogenous labeling like fluorescent dyes or targeted probes. This non-invasive approach avoids potential toxicity or imaging delay issues caused by contrast agents, making it particularly suitable for precise molecular identification<sup>56</sup>.

Recent advancements in Raman imaging have focused on its integration with other imaging modalities to overcome some of its limitations, such as low signal intensity. One promising development is the combination of surface-enhanced resonance Raman scattering (SERRS) with multispectral optoacoustic tomography (MSOT) for the precise delineation of brain tumors<sup>55</sup>. This dual-modality approach leverages the high sensitivity of SERRS with the deep-tissue imaging capabilities of MSOT, offering a new pathway for improving the accuracy of brain tumor resection<sup>55</sup>. Similarly, fluorescence-Raman bimodal nanoprobes that selectively accumulate in tumor tissues are enabling real-time fluorescence imaging for tumor detection, followed by Raman-based verification, thus expanding the scope of nanoprobes into therapeutic applications<sup>56</sup>. While combining with MRI-radiomics features for transperineal prostate cancer detection, it can also enhance the accuracy of cancer detection<sup>57</sup>.

Moreover, a recent clinical study explored the integration of Raman spectroscopy in head and neck cancer surgeries, where intraoperative spectral acquisition times were reduced to as low as 2 min after initial learning phases<sup>58</sup>. This development demonstrates the potential of Raman systems in surgical settings, addressing the challenge of longer acquisition times and making them more feasible for real-time application.

Thus, the primary advantage of Raman imaging technology is its ability to provide highly specific and sensitive molecular imaging without the need for non-invasive tissue analysis, complementing the shortcomings of NIR, PAI, and other technologies at the chemical molecular level to some extent. Additionally, Raman imaging can offer high-resolution images of deep tissues, aiding in precise tumor margin identification and staging. Furthermore, combining these advancements with deep learning algorithms could facilitate rapid and detailed pathological identification of cancer subtypes, differentiation grades, and tumor stages.

### 3D reconstruction

In recent advancements in medical imaging technology, the combination of three-dimensional (3D) imaging and fluorescence-guided surgery has emerged as a revolutionary approach to enhance the precision and effectiveness of surgical procedures. This technology leverages the capabilities of 3D image analysis and NIR fluorescence to provide surgeons with a detailed and real-time visualization of anatomical structures and pathological changes.

The initial application integrates a 3D medical image analyzer with infrared thoracoscopy for the purpose of pulmonary sublobar resection<sup>59</sup>. In these procedures, the use of transbronchial ICG instillation alongside infrared thoracoscopy has enhanced the visualization of the resection region, ensuring that the targeted area is accurately excised as per the preoperative simulation<sup>59</sup>. When it comes to LN dissection, fluorescence imaging combined with 3D lymphovascular reconstruction has been utilized in lateral pelvic node dissection for rectal cancer patients, leading to a 40.0% confirmation rate of pathological lateral pelvic node metastasis, emphasizing its role in identifying and removing metastatic nodes<sup>60</sup>.

Combining computer vision with endoscopy enables real-time 3D visualization of surgical sites, which can be crucial for navigating intricate surgical areas. A finding of a bio-inspired endoscope achieves simultaneous and real-time imaging of three-dimensional stereoscopic, color, and NIR fluorescence, providing surgeons with real-time feedback on tumor tissue and lymph nodes without impeding surgical workflow<sup>61</sup>. With a resolution of 7 lp/mm under visible illumination and 4 lp/mm under NIR, this system shows promise for use in image-guided and robotic surgery.

3D reconstruction technology does provide surgeons with a good spatial vision. However, there are challenges, such as the need for specialized equipment, the complexity of preoperative planning and intraoperative decision-making, and the potential for lower resolution in NIR imaging, which may affect the accuracy of fluorescent labeling.

### Multimodal imaging

Multimodal imaging, which combines two or more imaging techniques, overcomes the limitations of individual methods to provide complementary information, thus improving diagnostic accuracy and treatment outcomes. This approach allows for simultaneous characterization, visualization, and quantification of biological processes, making it highly beneficial for precision medicine. Each modality in the combination brings unique strengths to the table; for example, PET provides high sensitivity for metabolic activity, while CT offers precise anatomical delineation. Together, these modalities enable improved tumor localization and margin assessment, essential for successful tumor resection. For example, PET/CT imaging of colon and breast cancer has been utilized to provide both preoperative and intraoperative visualization, resulting in high sensitivity and spatial resolution for tumor delineation<sup>62,63</sup>.

Techniques such as PET/optical dual-modality imaging have also shown the potential to improve intraoperative guidance, offering more precise surgeries and better patient outcomes<sup>64</sup>. For example, PET/CT's strength in detecting metabolically active tissue complements the anatomical precision of CT, while techniques like fluorescence imaging combine functional imaging with structural detail, improving diagnostic and treatment outcomes<sup>65</sup>. Additionally, nanoparticles carrying multiple contrast agents have been developed to enhance the effectiveness of multimodal imaging, such as PET/MRI, combining the benefits of metabolic imaging with high-resolution anatomical imaging.

Challenges remain, however, including the complexity of data integration from different imaging modalities and the longer processing times involved. Recent innovations, such as the synergy between Raman spectroscopy, deep learning, and optical coherence tomography (OCT), show promise in enhancing real-time intraoperative diagnoses<sup>66,67</sup>. A study comparing OCT to conventional renal mass biopsy found that OCT offered superior diagnostic yield<sup>67</sup>, with a sensitivity of 91% and specificity of 56% for differentiating benign renal masses from renal cell carcinoma and a sensitivity of 92% and specificity of 67% for differentiating oncocytoma from renal cell carcinoma<sup>67</sup>. Combining imaging techniques can enhance tumor detection accuracy and facilitate precise tumor resection.

### Other imaging strategies

A range of innovative imaging technologies and platforms have been developed to enhance the precision and effectiveness of tumor detection and resection. One such innovation is the dual-functional Embolization-Visualization System integrates pre-surgical embolization with improved

visualization for endoscopic fluorescence image-guided tumor resection<sup>68</sup>. By utilizing silk-elastin-like protein polymers to deliver ICG for tumor margin marking and bleeding control, this system improves gross tumor resection and reduces surgical morbidity. Building on this, a modular theranostics platform that fluorescently visualizes hypoxia through light-modulated signal compensation, addressing tumor heterogeneity and serving as a diagnostic tool for image-guided surgical resection and photodynamic therapy<sup>25</sup>. This novel strategy significantly enhances hypoxia fluorescence imaging and therapeutic effects.

Another noteworthy development is an intelligent system that integrates a laser ablation module, optical coherence tomography unit, and a robotic arm to achieve automated lesion localization and laser ablation<sup>69</sup>. Demonstrating high precision in reaching planned positions and accuracy in tissue classification, this system exemplifies the potential for precise and intelligent theranostics, further expanding the capabilities of medical imaging in cancer treatment. While showcasing a high-sensitivity endoscopic Cerenkov luminescence imaging system, with its dual-mode deep cooling approach, can also enhance imaging sensitivity for detecting deep tumors, particularly hepatocellular carcinoma, and guide tumor resection effectively<sup>70</sup>. Additionally, studies on automated landmark detection for augmented reality in laparoscopic liver resection were conducted, identifying significant difficulties in manual landmark registration, particularly in transforming preoperative to intraoperative imaging environments. By leveraging a dataset of 167 laparoscopic images augmented by 3D models, these systems demonstrate efficacy in automated segmentation, although substantial barriers remain in robust segmentation of 3D landmarks<sup>70</sup>. Similarly, research on preoperative tumor size assessments in stage IB2 cervical cancer patients has underscored discrepancies in standard imaging methods, particularly MRI, and highlighted the need for more accurate preoperative evaluation to inform treatment decisions<sup>71</sup>.

These advancements illustrate the evolving landscape of medical imaging, where integrating various technologies enhances tumor detection, precision surgery, and overall patient outcomes. The synergy of these methods promises not only to refine surgical techniques but also to expand the scope of image-guided therapies in cancer treatment.

## Clinical applications

With the rapid advancement of imaging technologies, first-in-human trials have also seen a significant rise. Over the past five years, a diverse array of imaging techniques has been explored for intraoperative navigation, with clinical trials conducted across various tumor types, demonstrating promising outcomes and manageable complications (Table 2). The studies selected for inclusion in Table 2 were those that provided real-world applications of these technologies in human surgeries, with a specific focus on tumor resection and tumor margin identification.

Notably, Hu et al. (2020) demonstrated the impressive accuracy of NIR-II imaging in liver cancer, achieving a sensitivity of 100% and accuracy of 91.43% in liver cancer, with a superior tumor-to-normal-liver-tissue signal ratio compared to NIR-I (NIR-II 5.33 vs. NIR-I 1.45), especially in extrahepatic metastasis cases<sup>39</sup>. This improvement in imaging quality, combined with the technique's resistance to operating room lighting, underscores the robustness of NIR-II for clinical application. Zeng et al. (2024) study further validated NIR-II's potential, achieving 100% accuracy with B7H3-IRDye800CW in Osteosarcoma<sup>16</sup>, further proving NIR-II imaging's promising potential. This further solidifies NIR-II's promising role in precision tumor visualization, especially when coupled with multispectral channels to clarify anatomical and fluorescent structures and assist in sentinel lymph node detection. Yao et al. (2023) study demonstrated that incorporating V-EUS generated by a generative adversarial network could improve pocket-sized ultrasound's diagnostic performance by about 5% in breast cancer<sup>54</sup>, marking a significant step forward in traditional ultrasound imaging.

In clinical applications, imaging time remains a critical factor, making real-time visualization highly desirable during tumor-directed surgery. Although some advanced imaging modalities require complex and costly infrastructure, it is equally important to emphasize that many emerging

techniques discussed do not rely on invasive labeling and are not inherently associated with toxicity. Reports of transient adverse events, such as ALT elevation, highlight the need for continued optimization; however, these events are not universal across imaging platforms. Future developments should therefore aim to balance safety, minimal biological impact, and cost-effectiveness while maintaining the practicality and broad applicability of intraoperative imaging technologies.

## Limitations and future trends

### Technical limitations

Despite significant advances, intraoperative imaging technologies face several technical constraints that hinder their widespread clinical adoption, including high costs, complex equipment, and a steep learning curve for surgeons.

Firstly, many advanced modalities—such as NIR-II fluorescence imaging and multimodal systems—require bulky, expensive equipment and complex calibration procedures, limiting their use to high-resource centers. Real-time imaging at high resolution remains challenging due to hardware limitations, particularly in photoacoustic and Raman modalities, which suffer from slow acquisition speeds and low signal-to-noise ratios *in vivo*. To move the field forward, research should prioritize the miniaturization and portability of imaging platforms. Nevertheless, the accuracy of miniaturized handheld devices can be compromised by patient respiration, changes in position, and surgeon hand stability, requiring the integration of augmented reality technology to mitigate these errors<sup>72</sup>.

What's more, the integration of imaging data with surgical navigation systems lacks standardization, impeding seamless workflow. For example, fluorescence-guided systems often struggle with depth resolution and interference under ambient lighting, especially in open surgery. Use of specialized filters and advanced image processing algorithms can reduce the impact of ambient lighting on fluorescence imaging, techniques such as structured light illumination or time-of-flight imaging may also be a resolution ensuring clear and reliable visualization during open surgeries.

The toxicity associated with exogenous imaging agents remains a critical concern, emphasizing the need to achieve high-quality imaging with the minimal effective dose. Furthermore, standardized validation protocols across centers are needed to assess performance in diverse surgical settings, ensuring advanced technologies can compete with established gold standards.

### AI integration and smart imaging

Artificial intelligence (AI) is rapidly transforming various aspects of medicine, with intraoperative navigation being one of the areas where its impact is increasingly evident<sup>66</sup>. One key application is the real-time identification by enhancing tumor boundary detection and anatomical recognition. For example, machine learning combined with diffuse reflectance spectroscopy has achieved diagnostic accuracies above 93% in distinguishing cancerous from normal tissues in gastric and esophageal surgeries, enabling real-time feedback<sup>73</sup>. Building on this, deep learning models have been applied to identify critical structures—such as liver vasculature<sup>74</sup> and the hepatocystic triangle<sup>75</sup>—with high accuracy, improving safety in procedures like laparoscopic liver resection and cholecystectomy. Beyond structural recognition, AI models have shown strong performance in predicting lymph node metastasis status in pancreatic ductal adenocarcinoma<sup>76</sup>, thereby informing surgical planning and strategy during the operation, while potentially reducing the time and risk associated with waiting for intraoperative frozen pathology results. In addition to image recognition, AI aids probe design by predicting molecular properties<sup>77</sup>, expediting the development of stable and specific fluorescent agents for clinical use.

However, several limitations currently hinder the broader application of AI in intraoperative imaging. Most models are trained on single-center datasets, limiting their generalizability and highlighting the need for large-scale prospective validation. Additionally, the “black-box” nature of many AI algorithms raises concerns about interpretability, emphasizing the importance of developing explainable AI models. Lastly, the establishment

**Table 2 | Application of imaging techniques for intraoperative navigation on humans in the past five years**

Imaging technology	Tumor type	Probe/Agents	Imaging time	Accuracy	Sensitivity	Specificity	Publication year
NIR-II fluorescence imaging	Liver tumor	ICG	Real-time (500 ms)	1.43% (76.9–98.2%)	100% (89.1–100%)	88.46%	2020 <sup>39</sup>
NIR-II fluorescence imaging	Osteosarcoma	B7H3-IRDye800CW	Real-time (30 ms at 1000 nm, 1 s at 1200 nm)	100%	NA	NA	2024 <sup>16</sup>
NIR-I fluorescence imaging	Liver tumor	ICG	Real-time (300 ms)	82.86% (66.4–93.4%)	90.63% (75.0%–98.0%)	88.46%	2020 <sup>39</sup>
Hexachromatic NIR fluorescence imaging	Breast cancer & Prostate cancer	ICG & MB	Real-time	92%	84%	100%	2021 <sup>47</sup>
NIR Fluorescence imaging	Vulvar cancer	<sup>99m</sup> Tc nanocolloid tracer	Real-time	NA	NA	NA	2023 <sup>3</sup>
NIR Fluorescence imaging	Liver cell cancer	ICG-HAS	Real-time	NA	NA	NA	2024 <sup>4</sup>
NIR Fluorescence imaging	Ovarian cancer	Pafolacianine (OTL-38)	Real-time	NA	83%	75.20%	2022 <sup>39</sup>
NIR Fluorescence imaging	Non-small-cell lung cancer & pulmonary metastases	Pafolacianine (OTL-38)	Real-time	NA	76.5% (66.7–84.2%)	74.10%	2023 <sup>30</sup>
NIR Fluorescence imaging	Non-small-cell lung cancer (stage I-II) & pulmonary metastases	Pafolacianine (OTL-38)	Real-time	NA	NA	NA	2025 <sup>78</sup>
Pegulicainine fluorescence-guided surgery	Breast cancer	Pegulicainine	Real-time	NA	76.30%	70.40%	2022 <sup>81</sup>
Pegulicainine fluorescence-guided surgery	Breast cancer	Pegulicainine	Real-time	NA	49.3% (37.0–61.6%)	85.2% (83.7–86.6%)	2023 <sup>32</sup>
Fluorescence imaging	Pituitary neuroendocrine tumors	Bevacizumab-800CW	Real-time	22%	NA	NA	2024 <sup>20</sup>
Fluorescence imaging (cyanine-5 fluorescence camera)	Penile squamous cell carcinoma	EMI-137 (c-MET receptor targeting tracer)	Real-time	100%	NA	NA	2022 <sup>17</sup>
PET/CT & Fluorescence imaging	Prostate cancer	<sup>68</sup> Ga-P3	Real-time	100%	79.1%	90.4%	2025 <sup>85</sup>
SPECT/CT & Fluorescence Imaging	Primary prostate cancer	<sup>99m</sup> Tc-PSMA & ICG DROP-IN gamma probe	NA	NA	NA	NA	2023 <sup>28</sup>
Virtual elastography ultrasound generated by GAN	Breast cancer	NA	Real-time	NA	NA	NA	2023 <sup>84</sup>
Raman spectroscopy	Head and neck squamous cell carcinoma	Label-free	2 min	NA	NA	NA	2025 <sup>38</sup>

GAN generative adversarial network, HSA human serum albumin, ICG Indocyanine green, MB methylene blue, NIR Near infrared, PSMA Prostate-specific membrane antigen, Tc Technetium, TMR Tumor-to-normal-liver-tissue signal ratio, V-EUS Virtual elastography ultrasound.

of clear ethical and regulatory frameworks is essential to ensure safe and responsible integration of AI into clinical practice.

### Personalized and precision medicine

Incorporating imaging technologies into personalized and precision medicine represents a critical frontier in oncologic surgery. Future advancements are likely to focus on integrating genetic and molecular profiling with intraoperative imaging to tailor surgical interventions for individual patients. Personalized imaging, which accounts for the unique molecular characteristics of each patient's tumor, could guide surgical interventions with greater specificity and accuracy. For example, the use of highly targeted probes can facilitate more precise localization of tumors based on their unique molecular signatures, thus enabling tailored resection strategies that align with each patient's specific disease profile. Furthermore, combining imaging data with genomic information could support the development of individualized treatment plans that minimize collateral damage to healthy tissues while maximizing the efficacy of tumor removal<sup>1</sup>.

### Conclusion

The emergence of novel imaging strategies for intraoperative navigation imaging represents a significant shift in oncologic surgery. Techniques such as fluorescence imaging, photoacoustic imaging, and multimodal imaging are enhancing tumor resection precision, improving patient outcomes, and reducing recurrence rates. These advanced tools, when integrated with conventional imaging methods, offer a more comprehensive approach to intraoperative navigation, allowing for better identification of tumor margins delineation and minimizing damage to surrounding healthy tissues.

Looking ahead, the integration of AI and machine-learning algorithms into imaging systems will further refine image analysis, enhancing surgical decision-making and providing real-time support for surgeons. Personalized and precision medicine will be further enabled by the combination of genetic and molecular profiling with intraoperative imaging, leading to tailored surgical interventions that are customized to individual patients' unique tumor profiles. However, challenges remain, including the high costs, complexity of equipment, and accessibility of these advanced technologies. Addressing these challenges is crucial for ensuring that these imaging strategies become the standard of care in cancer surgery worldwide. As innovation in this field continues, these imaging strategies will undoubtedly play a critical role in shaping the future of cancer diagnosis and treatment, offering hope for better patient outcomes and survival rates.

### Data availability

No datasets were generated or analyzed during the current study.

Received: 19 May 2025; Accepted: 26 February 2026;

Published online: 25 March 2026

### References

- Bray, F. et al. Global cancer statistics 2022: GLOBOCAN estimates of incidence and mortality worldwide for 36 cancers in 185 countries. *CA Cancer J. Clin.* **74**, 229–263 (2024).
- GBD 2016 Causes of Death Collaborators Global, regional, and national age-sex specific mortality for 264 causes of death, 1980–2016: a systematic analysis for the Global Burden of Disease Study 2016. *Lancet* **390**, 1151–1210 (2017).
- Ditto, A. et al. Real-time fluorescent ICG and 99m-Tc nanocolloid tracer navigation in bilateral sentinel lymph node mapping of vulvar cancer. *J. Minim. Invasive Gynecol.* **30**, 780–781 (2023).
- Gao, F. et al. Use of indocyanine green-human serum albumin complexes in fluorescence image-guided laparoscopic anatomical liver resection: a case series study (with video). *Surg. Endosc.* <https://doi.org/10.1007/s00464-024-11295-8> (2024).
- Shou, K. et al. Diketopyrrolopyrrole-based semiconducting polymer nanoparticles for in vivo second near-infrared window imaging and image-guided tumor surgery. *Chem. Sci.* **9**, 3105–3110 (2018).
- Azari, F. et al. Intraoperative molecular imaging clinical trials: a review of 2020 conference proceedings. *J. Biomed. Opt.* **26**, <https://doi.org/10.1117/1.JBO.26.5.050901> (2021).
- Wang, Y. et al. Application of near-infrared fluorescence imaging in the accurate assessment of surgical margins during breast-conserving surgery. *World J. Surg. Oncol.* **20**, 357 (2022).
- Nicoli, F. et al. Intraoperative near-infrared fluorescence (NIR) imaging with indocyanine green (ICG) can identify bone and soft tissue sarcomas which may provide guidance for oncological resection. *Ann. Surg.* **273**, e63–e68 (2021).
- Jeon, O. H. et al. Optimization of indocyanine green for intraoperative fluorescent image-guided localization of lung cancer; analysis based on solid component of lung nodule. *Cancers (Basel)* **15**, <https://doi.org/10.3390/cancers15143643> (2023).
- Yuda, M. et al. Appropriate concentration setting for the intraoperative administration of indocyanine green for fluorescence imaging to identify the sentinel lymph node in early gastric cancer: a clinical pilot study. *Surg. Today* **54**, 801–806 (2024).
- Midha, A., Dearden, S. & McCormack, R. EGFR mutation incidence in non-small-cell lung cancer of adenocarcinoma histology: a systematic review and global map by ethnicity (mutMapII). *Am. J. Cancer Res.* **5**, 2892–2911 (2015).
- Li, C. et al. New and effective EGFR-targeted fluorescence imaging technology for intraoperative rapid determination of lung cancer in freshly isolated tissue. *Eur. J. Nucl. Med. Mol. Imaging* **50**, 494–507 (2023).
- AghaAmiri, S. et al. Comparison of HER2-targeted antibodies for fluorescence-guided surgery in breast cancer. *Mol. Imaging* **2021**, 5540569 (2021).
- Lenárt, S. et al. Trop2: Jack of all trades, master of none. *Cancers (Basel)* **12**, <https://doi.org/10.3390/cancers12113328> (2020).
- Chen, W. et al. Intraoperative evaluation of tumor margins using a TROP2 near-infrared imaging probe to enable human breast-conserving surgery. *Sci. Transl. Med.* **16**, eado2461 (2024).
- Zeng, F. et al. Intraoperative resection guidance and rapid pathological diagnosis of osteosarcoma using B7H3 targeted probe under NIR-II fluorescence imaging. *Adv. Sci. (Weinh.)* **11**, e2310167 (2024).
- Vries, H. M. et al. c-MET receptor-targeted fluorescence on the road to image-guided surgery in penile squamous cell carcinoma patients. *J. Nucl. Med.* **63**, 51–56 (2022).
- Goto, M. et al. Image-guided surgery with a new tumour-targeting probe improves the identification of positive margins. *EBioMedicine* **76**, 103850 (2022).
- Miller, S. E. et al. First-in-human intraoperative near-infrared fluorescence imaging of glioblastoma using cetuximab-IRDye800. *J. Neurooncol.* **139**, 135–143 (2018).
- Schmidt, I. et al. Fluorescence detection of pituitary neuroendocrine tumour during endoscopic transsphenoidal surgery using bevacizumab-800CW: a non-randomised, non-blinded, single centre feasibility and dose finding trial [DEPARTURE trial]. *Eur. J. Nucl. Med. Mol. Imaging* <https://doi.org/10.1007/s00259-024-06947-9> (2024).
- Cheng, Z. et al. Fibronectin-targeting and metalloproteinase-activatable smart imaging probe for fluorescence imaging and image-guided surgery of breast cancer. *J. Nanobiotechnol.* **21**, 112 (2023).
- Lin, W. et al. Indocyanine green fluorescence image-guided laparoscopic anatomical S2/3 resection using the TICGL technique. *Surg. Endosc.* **38**, 1069–1076 (2024).
- Linders, D. G. J. et al. Ex vivo fluorescence-guided resection margin assessment in breast cancer surgery using a topically applied, cathepsin-activatable imaging agent. *Pharm. Res.* **209**, 107464 (2024).
- Xu, Y. et al. In Situ albumin-hitchhiking NIR-II probes for accurate detection of micrometastases. *Nano Lett.* **23**, 5731–5737 (2023).

25. Liu, W. et al. Modularized supramolecular assemblies for hypoxia-activatable fluorescent visualization and image-guided theranostics. *Theranostics* **14**, 3634–3652 (2024).
26. Baart, V. M. et al. Side-by-side comparison of uPAR-targeting optical imaging antibodies and antibody fragments for fluorescence-guided surgery of solid tumors. *Mol. Imaging Biol.* **25**, 122–132 (2023).
27. Yang, J. et al. Gold/alpha-lactalbumin nanoprobes for the imaging and treatment of breast cancer. *Nat. Biomed. Eng.* **4**, 686–703 (2020).
28. de Barros, H. A., van Oosterom, M. N., van Leeuwen, F. W. B., van der Poel, H. G. & van Leeuwen, P. J. Real-time identification of nodal metastases with 99m Tc-prostate-specific membrane antigen-based radioguidance and indocyanine green fluorescence imaging in primary prostate cancer surgery—on the road to hybrid image-guided surgery. *Clin. Nucl. Med.* **48**, 697–698 (2023).
29. Tanyi, J. L. et al. A Phase III study of pafolacianine injection (OTL38) for intraoperative imaging of folate receptor-positive ovarian cancer (Study 006). *J. Clin. Oncol.* **41**, 276–284 (2023).
30. Sarkaria, I. S. et al. Pafolacianine for intraoperative molecular imaging of cancer in the lung: the ELUCIDATE trial. *J. Thorac. Cardiovasc. Surg.* **166**, e468–e478 (2023).
31. Hwang, E. S. et al. Clinical impact of intraoperative margin assessment in breast-conserving surgery with a novel pegulicianine fluorescence-guided system: a nonrandomized controlled trial. *JAMA Surg.* **157**, 573–580 (2022).
32. Smith, B. L. et al. Intraoperative fluorescence guidance for breast cancer lumpectomy surgery. *NEJM Evid.* **2**, EVIDo2200333 (2023).
33. Pal, R. et al. Fluorescence lifetime of injected indocyanine green as a universal marker of solid tumours in patients. *Nat. Biomed. Eng.* **7**, 1649–1666 (2023).
34. Pal, R. et al. First clinical results of fluorescence lifetime-enhanced tumor imaging using receptor-targeted fluorescent probes. *Clin. Cancer Res.* **28**, 2373–2384 (2022).
35. Pal, R., Kang, H., Choi, H. S. & Kumar, A. T. N. Fluorescence lifetime-based tumor contrast enhancement using an EGFR antibody-labeled near-infrared fluorophore. *Clin. Cancer Res.* **25**, 6653–6661 (2019).
36. Shi, X., Cao, C., Zhang, Z., Tian, J. & Hu, Z. Radiopharmaceutical and Eu(3+) doped gadolinium oxide nanoparticles mediated triple-excited fluorescence imaging and image-guided surgery. *J. Nanobiotechnol.* **19**, 212 (2021).
37. Zhang, B. et al. Injectable and sprayable fluorescent nanoprobe for rapid real-time detection of human colorectal tumors. *Adv. Mater.* **36**, e2405275 (2024).
38. Zhang, Z. et al. NIR-II light in clinical oncology: opportunities and challenges. *Nat. Rev. Clin. Oncol.* **21**, 449–467 (2024).
39. Hu, Z. et al. First-in-human liver-tumour surgery guided by multispectral fluorescence imaging in the visible and near-infrared-I/II windows. *Nat. Biomed. Eng.* **4**, 259–271 (2020).
40. Zhou, H. et al. Upconversion NIR-II fluorophores for mitochondria-targeted cancer imaging and photothermal therapy. *Nat. Commun.* **11**, 6183 (2020).
41. Tian, R. et al. Multiplexed NIR-II probes for lymph node-invaded cancer detection and imaging-guided surgery. *Adv. Mater.* **32**, e1907365 (2020).
42. Lin, L. & Wang, L. V. The emerging role of photoacoustic imaging in clinical oncology. *Nat. Rev. Clin. Oncol.* **19**, 365–384 (2022).
43. Yu, Q. et al. Label-free visualization of early cancer hepatic micrometastasis and intraoperative image-guided surgery by photoacoustic imaging. *J. Nucl. Med.* **61**, 1079–1085 (2020).
44. Liu, Y., Gao, D., Xu, M. & Yuan, Z. Multispectral photoacoustic imaging of cancer with broadband CuS nanoparticles covering both near-infrared I and II biological windows. *J. Biophotonics* **12**, e201800237 (2019).
45. Yao, J. et al. Multiscale photoacoustic tomography using reversibly switchable bacterial phytochrome as a near-infrared photochromic probe. *Nat. Methods* **13**, 67–73 (2016).
46. Chen, P. et al. Aggregation-induced emission probe for fluorescence/photoacoustic dual-modality imaging and photodynamic/photothermal treatment. *Chem. Res. Chin. Univ.* **40**, 293–304 (2024).
47. Blair, S. et al. Hexachromatic bioinspired camera for image-guided cancer surgery. *Sci. Transl. Med.* **13**, <https://doi.org/10.1126/scitranslmed.aaw7067> (2021).
48. Garcia, M. et al. Bio-inspired imager improves sensitivity in near-infrared fluorescence image-guided surgery. *Optica* **5**, 413–422 (2018).
49. Jin, N. et al. Multispectral fluorescence imaging of EGFR and PD-L1 for precision detection of oral squamous cell carcinoma: a preclinical and clinical study. *BMC Med.* **22**, 342 (2024).
50. Sato, D. et al. Distinction of surgically resected gastrointestinal stromal tumor by near-infrared hyperspectral imaging. *Sci. Rep.* **10**, 21852 (2020).
51. Schimunek, L. et al. Hyperspectral imaging as a new diagnostic tool for cervical intraepithelial neoplasia. *Arch. Gynecol. Obstet.* **308**, 1525–1530 (2023).
52. Aboughaleb, I. H., Aref, M. H. & El-Sharkawy, Y. H. Hyperspectral imaging for diagnosis and detection of ex-vivo breast cancer. *Photodiagn. Photodyn. Ther.* **31**, 101922 (2020).
53. Gillies, D. J. et al. Geometrically variable three-dimensional ultrasound for mechanically assisted image-guided therapy of focal liver cancer tumors. *Med. Phys.* **47**, 5135–5146 (2020).
54. Yao, Z. et al. Virtual elastography ultrasound via generative adversarial network for breast cancer diagnosis. *Nat. Commun.* **14**, 788 (2023).
55. Neuschmelting, V. et al. Dual-modality surface-enhanced resonance Raman scattering and multispectral optoacoustic tomography nanoparticle approach for brain tumor delineation. *Small* **14**, e1800740 (2018).
56. Pal, S. et al. DNA-enabled rational design of fluorescence-Raman bimodal nanoprobes for cancer imaging and therapy. *Nat. Commun.* **10**, 1926 (2019).
57. Grajales Lopera, D. O. et al. Image-guided Raman spectroscopy navigation system to improve transperineal prostate cancer detection. Part 2: in-vivo tumor-targeting using a classification model combining spectral and MRI-radiomics features. *J. Biomed. Opt.* **27**, <https://doi.org/10.1117/1.Jbo.27.9.095004> (2022).
58. Bali, A. et al. Establishment of a clinical workflow for in vivo Raman spectroscopy during head and neck cancer surgery. *Sci. Rep.* **15**, 24230 (2025).
59. Sekine, Y. et al. Precise anatomical sublobar resection using a 3D medical image analyzer and fluorescence-guided surgery with transbronchial instillation of indocyanine green. *Semin. Thorac. Cardiovasc. Surg.* **31**, 595–602 (2019).
60. Kim, H. J. et al. S122: impact of fluorescence and 3D images to completeness of lateral pelvic node dissection. *Surg. Endosc.* **34**, 469–476 (2020).
61. Liu, C. et al. Bio-inspired multimodal 3D endoscope for image-guided and robotic surgery. *Opt. Express* **29**, 145–157 (2021).
62. Jing, B. et al. Extracellular vesicles-based pre-targeting strategy enables multi-modal imaging of orthotopic colon cancer and image-guided surgery. *J. Nanobiotechnol.* **19**, 151 (2021).
63. De Crem, A. S. et al. Breast cancer intraoperative margin assessment using specimen PET-CT (BIMAP). *NPJ Breast Cancer* **11**, 101 (2025).
64. Shi, S. et al. In vivo tumor-targeted dual-modality PET/optical imaging with a yolk/shell-structured silica nanosystem. *Nanomicro Lett.* **10**, 65 (2018).
65. Chen, S. et al. First-in-human study of a dual-modality prostate-specific membrane antigen-targeted probe for preoperative positron emission tomography/computed tomography imaging and intraoperative fluorescence imaging in prostate cancer. *Eur. Urol.* **87**, 717–727 (2025).
66. Huang, L. et al. Rapid, label-free histopathological diagnosis of liver cancer based on Raman spectroscopy and deep learning. *Nat. Commun.* **14**, 48 (2023).

67. Buijs, M. et al. An in-vivo prospective study of the diagnostic yield and accuracy of optical biopsy compared with conventional renal mass biopsy for the diagnosis of renal cell carcinoma: the interim analysis. *Eur. Urol. Focus* **4**, 978–985 (2018).
68. Jensen, M. M. et al. A dual-functional embolization-visualization system for fluorescence image-guided tumor resection. *Theranostics* **10**, 4530–4543 (2020).
69. Li, Y. et al. Intelligent optical diagnosis and treatment system for automated image-guided laser ablation of tumors. *Int. J. Comput. Assist. Radiol. Surg.* **16**, 2147–2157 (2021).
70. Zhang, Z., Cai, M., Bao, C., Hu, Z. & Tian, J. Endoscopic Cerenkov luminescence imaging and image-guided tumor resection on hepatocellular carcinoma-bearing mouse models. *Nanomedicine* **17**, 62–70 (2019).
71. Pan, T. L. et al. Accuracy of pre-operative tumor size assessment compared to final pathology and frequency of adjuvant treatment in patients with FIGO 2018 stage IB2 cervical cancer. *Int. J. Gynecol. Cancer* <https://doi.org/10.1136/ijgc-2024-005986> (2024).
72. Han, Z. & Dou, Q. A review on organ deformation modeling approaches for reliable surgical navigation using augmented reality. *Comput. Assist. Surg. (Abingdon)* **29**, 2357164 (2024).
73. Nazarian, S. et al. Real-time tracking and classification of tumor and nontumor tissue in upper gastrointestinal cancers using diffuse reflectance spectroscopy for resection margin assessment. *JAMA Surg.* **157**, e223899 (2022).
74. Une, N. et al. Intraoperative artificial intelligence system identifying liver vessels in laparoscopic liver resection: a retrospective experimental study. *Surg. Endosc.* **38**, 1088–1095 (2024).
75. Madani, A. et al. Artificial intelligence for intraoperative guidance: using semantic segmentation to identify surgical anatomy during laparoscopic cholecystectomy. *Ann. Surg.* **276**, 363–369 (2022).
76. Chu, L. C. & Fishman, E. K. Artificial intelligence outperforms radiologists for pancreatic cancer lymph node metastasis prediction at CT. *Radiology* **306**, 170–171 (2023).
77. Xiang, F. F. et al. Machine-learning-assisted rational design of Si horizontal line rhodamine as cathepsin-pH-activated probe for accurate fluorescence navigation. *Adv. Mater.* **36**, e2404828 (2024).
78. Rice, D. et al. Intraoperative molecular imaging with pafolacianine in resection of occult pulmonary malignancy in the ELUCIDATE trial. *Ann. Thorac. Surg.* **120**, 294–301 (2025).

## Acknowledgements

Figure 1 was created with biorender.com. This work was supported by the National Key Research and Development Program of China (2024YFC3405303) and Natural Science Foundation of Beijing Municipality (7244427).

## Author contributions

All authors contributed to this review’s conception and design. Ke Li and Yiyin Zhang prepared the initial manuscript draft. Shu Wang and Houpu Yang commented on previous versions of the manuscript. Every author reviewed and endorsed the final version of this manuscript.

## Competing interests

The authors declare no competing interests.

## Additional information

**Correspondence** and requests for materials should be addressed to Shu Wang.

**Reprints and permissions information** is available at <http://www.nature.com/reprints>

**Publisher’s note** Springer Nature remains neutral with regard to jurisdictional claims in published maps and institutional affiliations.

**Open Access** This article is licensed under a Creative Commons Attribution-NonCommercial-NoDerivatives 4.0 International License, which permits any non-commercial use, sharing, distribution and reproduction in any medium or format, as long as you give appropriate credit to the original author(s) and the source, provide a link to the Creative Commons licence, and indicate if you modified the licensed material. You do not have permission under this licence to share adapted material derived from this article or parts of it. The images or other third party material in this article are included in the article’s Creative Commons licence, unless indicated otherwise in a credit line to the material. If material is not included in the article’s Creative Commons licence and your intended use is not permitted by statutory regulation or exceeds the permitted use, you will need to obtain permission directly from the copyright holder. To view a copy of this licence, visit <http://creativecommons.org/licenses/by-nc-nd/4.0/>.

© The Author(s) 2026